16th World Conference on Earthquake, 16WCEE 2017

Santiago Chile, January 9th to 13th 2017

Paper N° 2257

Registration Code: S-H1461857839

FEASIBILITY OF HYSTERETIC ENERGY DISSIPATORS FOR BULK SEISMIC PROTECTION OF VULNERABLE BUILDINGS IN CHILE

D. Domínguez(1), F. López-Almansa(2)

(1) *Associate Professor, University of Talca, ddominguez@utalca.cl*

(2) *Professor, Technical University of Catalonia, francesc.lopez-almansa@upc.edu*

Abstract

This paper explores the viability of using energy dissipators for implementing earthquake-resistant measures for common vulnerable buildings in Chile. Hysteretic devices (e.g. based on plastification of metals) are considered. This study deals both with design of new buildings and retrofit of existing ones. Three 3, 5 and 10-story RC buildings are analyzed; each building is designed for five situations: no seismicity, rock soil in seismic zone 3 in Chile with full/reduced seismicity, and soft soil in the same zone with full/reduced seismicity. The behavior of these buildings is analyzed in terms of modal parameters and capacity curves (after pushover analyses). The seismicity is characterized in terms of input and hysteretic energy; using this information, the optimal design parameters of the dissipative devices are obtained.

Keywords: Energy Dissipators; Hysteretic Devices; Energy-Based Design

1. Introduction

A relevant number of buildings in Chile are highly vulnerable to strong earthquakes due mainly to lack of design requirements of the past design codes, and, less intensively, to construction deficiencies and to the high uncertainty inherent in the important Chilean seismicity. Several design and retrofit solutions have been proposed; they can be broadly grouped in traditional and innovative strategies.

Traditional techniques consist principally in designing resistant, stiff and ductile structures. These solutions have shown repeatedly their efficiency in reducing damage after strong seismic events; however, major objections exist: (i) cost is, in general, excessive, (ii) architectural and functional impact is important, and, mainly, (iii) since ductility is provided by the structure itself, in case of strong excitations, damage is concentrated in the structural elements, thus preventing any post-event reusability. To cope with these limitations, two main innovative approaches have been proposed: base isolation and energy dissipation.

Base (seismic) isolation consists in incorporating to the building foundation elements which are highly flexible in the horizontal direction (commonly termed as isolators). In this way, the building is flexibilized (the fundamental period is dramatically elongated) and is essentially uncoupled from the horizontal ground motion; therefore, the design base shear force is markedly reduced. Another relevant advantage is that, since most of strain is concentrated in the isolation layer, the incorporation of additional damping is highly feasible. Base isolation has been deeply investigated and many applications have been reported, particularly in Chile. Noticeably, a number of isolated buildings have performed satisfactorily under strong earthquakes, thus confirming the efficiency of this solution. Nevertheless, seismic isolation still have some major limitations: (i) the isolators must be able to resist the weight of the building, therefore the use of simple elements as isolators is prevented, (ii) this technology cannot be considered for high rise buildings, because of the important weight to be resisted and because of the long fundamental period of the tall fixed-base buildings, (iii) the use of base isolation on soft soil is controversial due to the relevant soil-structure interaction effects, (iv) the permanent input displacements near to active faults can be enormous, thus forcing to design huge isolators, and (v) isolation is not effective against wind gusts.

Energy dissipators constitute another innovative strategy, overcoming most of the limitations of base isolation. Energy dissipators are devices external to the main structural system, in the sense that they do not participate in the gravity-load-carrying system. They are connected to the structure in such a way as experience important deformations under interstory drift motions, as shown by Fig. 1. Through these deformations, the dissipators absorb energy, thus protecting the rest of the construction; said in a clearer way, they can be considered as "structural fuses" (i.e. the "weakest links") of the structural chain. Furthermore, these elements can

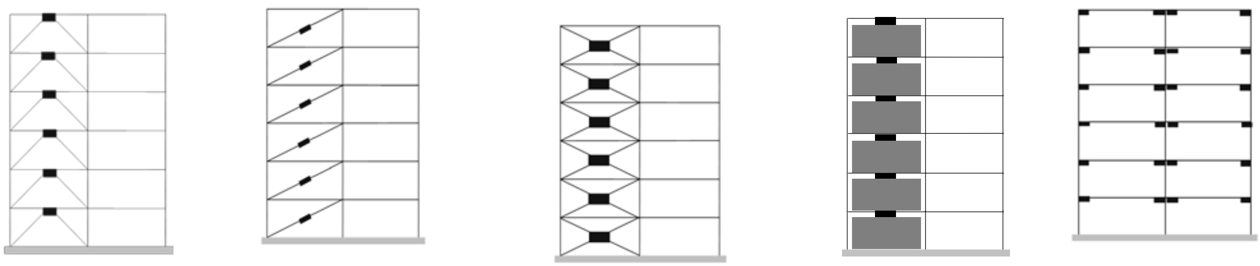

(a) Chevron braces (b) Diagonal braces (c) Double diagonal braces (d) Infill walls (e) Beam-column joints

Fig. 1 – Layout of energy dissipators for seismic protection of framed buildings

be easily replaced after having being damaged by strong earthquakes.

Fig. 1 shows that, in most of the cases, the energy dissipators for seismic protection of building structures are connected to the main frame either through additional bracing systems (Fig. 1.a through Fig. 1.c) or through RC or masonry infill walls (Fig. 1.d). Therefore, the seismic efficiency of the dissipators must be judged by comparing three major design solutions: (i) **bare** (conventional frame or dual structure, without any bracing), (ii) **protected** (frame with dissipative devices as shown in Fig. 1), and (iii) **braced** (conventional frame with steel diagonal or chevron braces rigidly connected to the main structure, instead of through dissipators, as shown in Fig. 1).

As discussed previously, comparison with base isolation shows that energy dissipators have some advantages: (i) they do not need to resist the building weight, therefore, extremely simple elements can be used, (ii) dissipators can be considered either for low, mid and high rise buildings, (iii) dissipators are not strongly coupled to the soil parameters, (iv) the near-fault effects do not affect to the dissipators as directly as to the isolators, and (v) dissipators can be effective against wind gusts. Noticeably, since very simple dissipative devices can be considered, this technology can be particularly effective for bulk use, even in developing countries. Energy dissipators have been proposed both for new constructions and for retrofit, and a relevant number of applications has been reported; in Chile, dissipators have been only considered for seismic protection of new constructions. A number of buildings equipped with dissipative devices have experienced strong seismic inputs and have performed satisfactorily; in Chile the Titanium building (La Portada) in Santiago behaved properly under the Maule 2010 earthquake. In Chile there has been previous research on energy dissipators [1-2].

The hitherto proposed devices can be classified with respect to their dissipation mechanisms into: hysteretic (yielding of metals), friction, viscoelastic materials, viscous fluids, super-elasticity (shape memory alloys), and other mechanisms. The hysteretic devices can provide excellent performance yet being significantly cheaper and simpler than the other dissipators and have little maintenance requirements. For this reason, this research focusses exclusively on hysteretic dissipators, aiming to its massive use. These devices are better suited for chevron bracing (Fig. 1.a) and walls (Fig. 1.d); therefore, both solutions are considered in this research, although the first one is preferred.

This work is a part of a wider research effort aiming to contribute to the extensive use of hysteretic energy dissipators, both for seismic retrofit of existing buildings and for new constructions, to reduce the seismic vulnerability of buildings in Chile. This paper presents the early stages of this research; it comprises the selection of three representative prototype buildings and the design of energy dissipative devices.

2. Prototype buildings

2.1 General considerations

Three 3, 5 and 10-story RC prototype buildings are selected to represent a relevant fraction of the vulnerable buildings in Chile. These buildings are located in seismic zone 3 [3] (A_0 = 0.4 g, the highest) for two soil types: A (rock, $v_{s,30} \geq 900$ m/s) and D (soft, 180 m/s $\leq v_{s,30} \leq$ 350 m/s). As discussed in section 1, the objective of this work is to compare the use of hysteretic energy dissipators with competing traditional design and retrofit solutions; therefore, the main structure of each building is designed for four groups of seismic demand conditions:

1. Frame or dual structure (there are neither energy dissipators nor bracing, but structural walls can be used) founded on rock/soft soil and located in seismic zone 3. This case corresponds to "**bare**" solution in section 1.
2. Braced frame structure (chevron bracing) founded on rock/soft soil and located in seismic zone 3. This case corresponds to "**braced**" solution in section 1.
3. Frame structure founded on rock/soft soil and located in seismic zone 3 but with the design base shear reduced 25%. This case corresponds to "**protected**" solution in section 1 fulfilling ASCE 7/10 [4]. ASCE 7/10 considers the dissipators rather as an additional safety measure and, therefore, states that the main structure alone (i.e. without the cooperation of the damping system) has to be designed to resist at least seismic forces corresponding to 75% of the base shear for the bare structure.
4. Frame structure without any seismic consideration. This case corresponds to "**protected**" solution in section 1 not fulfilling ASCE 7/10 [4]. This solution relies entirely on the seismic resistance of the energy dissipation system; it is included to highlight the consequences of the allegedly excessive conservatism of ASCE code.

According to this list, prototype buildings are grouped next in: bare frame (1), bare dual (1), braced frame (2), protected frame with reduced base shear (3) and protected frame (4). Given that each type of building (except the last one) can be designed for rock and for soft soil, and there are buildings with 3, 5 and 10 levels, the number of analyzed buildings is $(2 + 2 + 2 + 2 + 1) \times 3 = 27$.

Noticeably, to provide realistic comparisons, in each case the structure is designed looking for the best solution independently of the other cases. It is also worth noting that the study is not focused on any particular type of hysteretic damper; conversely, the research is interned to be more general and cover any type of energy dissipator based on plastification of metals.

2.2 Description of the prototype buildings

The buildings have square plan configuration 20 m × 20 m. Structural walls or braces are placed whenever necessary for seismic resistance according the considerations in subsection 2.1. Fig. 2 displays plan views of buildings without (Fig. 2.a) and with (Fig. 2.b) walls.

Fig. 2 shows that each building has 25 columns and that slabs are formed by cast-in-situ column-to-column beams and slabs resting on their four sides. Span-length is 5 m, beams section ranges between 35 cm × 35 cm and 40 cm × 50 cm and slab depth is 12 cm. Following common construction practices in Chile, the roof is lighter. Columns have square section ranging between 30 cm × 30 cm and 60 cm × 60 cm; sections are changed every three or four stories (3 + 2 for the 5-story building and 4 + 3 + 3 for the 10-story one). Structural walls are 25 cm thick.

Prototype buildings are uniform along their height; first floor is 4 m high and other floors are 3 m high. Therefore, height of 3, 5 and 10-story buildings is 10, 16 and 31 m, respectively.

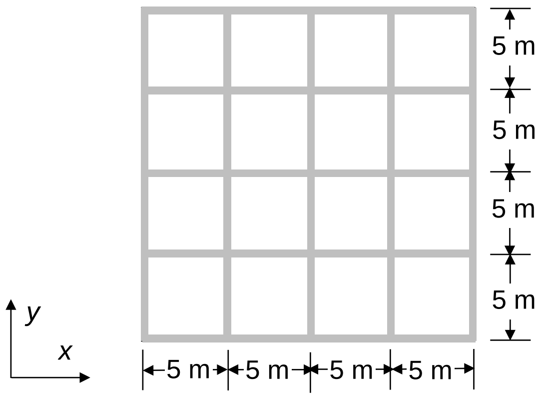

(a) Building without walls

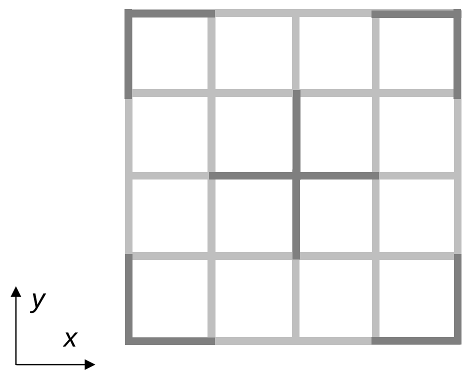

(b) Building with walls or braces

Fig. 2 – Plan layouts of the prototype buildings

2.3 Design of the prototype buildings

The prototype buildings are designed, as usual in Chile, following the Chilean codes [3,5-7] although are supplemented, wherever necessary, with the American regulations [8]. The use of the buildings is housing, administrative or equivalent. The characteristic value of the concrete compressive strength is f_c' = 30 MPa and the reinforcement steel yield point is f_{yk} = 500 MPa. Braces are made of steel grade A36 [9]. Braces are made with HSS (Hollow Square Section); section ranges between 80 mm × 3 mm and 100 mm × 40 mm; sections are changed every three or four stories (3 + 2 for the 5-story building and 3 + 3 + 4 for the 10-story one). Live load is L = 3 kN/m^2. The overall damping factor is 5%. Given that the structure is made of concrete, the response modification factor for simplified static analysis is R = 7; the factor for modal spectral analysis is R_0 = 11. In the braced buildings, the dimensionless slenderness of the braces is limited to 2 [10].

2.4 Structural modelling of the prototype buildings

The static and dynamic behavior of the prototype buildings is simulated with software package SeismoStruct [11]. Due to cracking of tensioned concrete, the initial stiffness of structural members is reduced; it is based on gross sectional parameters, but the concrete modulus of elasticity is reduced as indicated in [12]. The sectional behavior is based on the average properties of materials, instead on the characteristic ones; in case of concrete, average compressive strength is f_c = f_c' + 8 = 38 MPa [13]. The nonlinear behavior is represented by concentrated plasticity models based on plastic hinges located at member ends; the length of the plastic hinges is 15 cm [14,15]. Moment- curvature laws are bilinear; parameters are obtained after program XTRACT [16].

2.5 Behavior of the prototype buildings

For each prototype building, a linear modal analysis is carried out; seismic weight correspond to dead load and 30% of the live one. Table 1 and Table 2 display the fundamental period and the seismic weight of the prototype building, respectively; numbers in parenthesis correspond to list in subsection 2.1.

Table 1 – Fundamental period (s) of the prototype buildings

No. of stories	Bare (1)				Braced (2)		Protected (3, 4)		
	Frame		Dual				Frame for 75% of base shear (3)		Frame without seismic design (4)
	Rock	Soft soil	Rock	Soft soil	Rock	Soft soil	Rock	Soft soil	
3	0.46	0.38	0.096	0.093	0.303	0.264	0.48	0.45	0.605
5	0.70	0.61	0.14	0.13	0.35	0.327	0.80	0.67	0.77
10	1.00	0.85	0.23	0.22	0.604	0.527	1.40	1.12	1.26

Table 2 – Seismic weight (kN) of the prototype buildings

No. of stories	Bare (1)				Braced (2)		Protected (3, 4)		
	Frame		Dual				Frame for 75% of base shear (3)		Frame without seismic design (4)
	Rock	Soft soil	Rock	Soft soil	Rock	Soft soil	Rock	Soft soil	
3	9113	9804	11613	12304	9125	9823	8813	9600	8940
5	16754	17925	20754	21925	16782	17958	16075	17488	15150
10	36311	40481	44746	48915	36376	40553	35662	39071	33182

Static nonlinear (pushover) analysis are carried out using the numerical models described in subsection 2.4; second-order effects are accounted for by a P-delta analysis. The variation of the pushing forces along building height is triangular. Fig. 3, Fig. 5 and Fig. 6 display, in terms of base shear force vs. top floor displacement the obtained capacity curves for the 3, 5 and 10-story buildings, respectively. Fig. 4 displays capacity curves in terms of base shear coefficient (base shear force divided by building weight) vs. drift angle for the 3-story building.

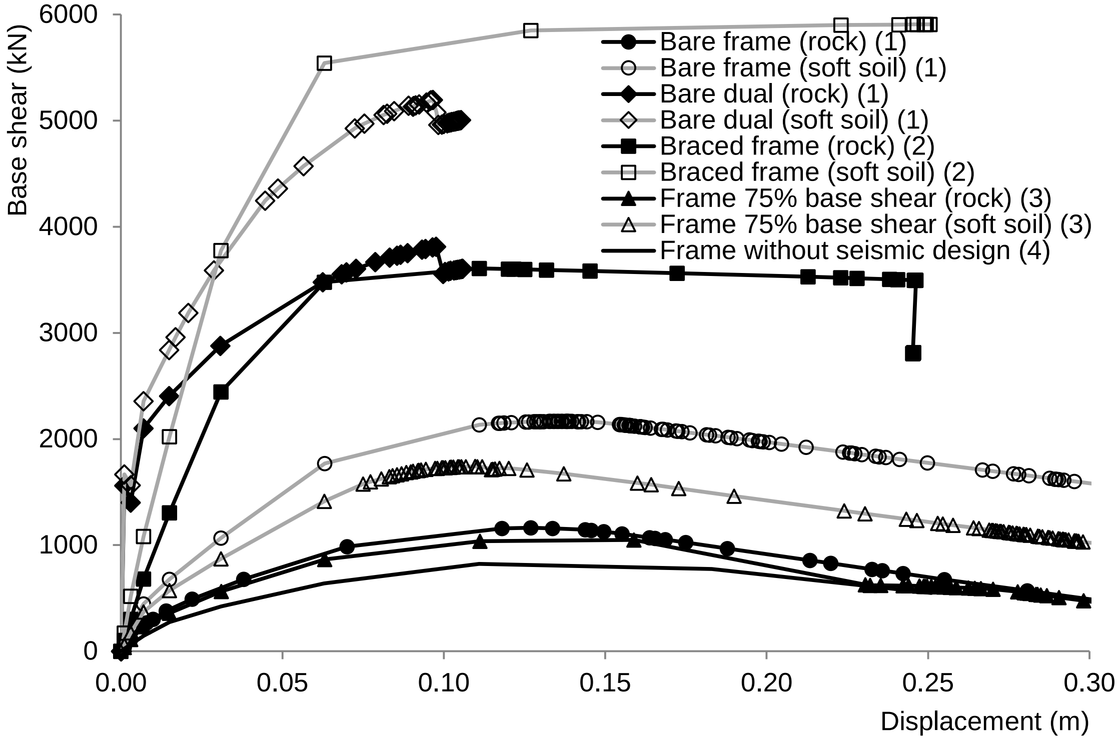

Fig. 3 – Capacity curves of the 3-story buildings

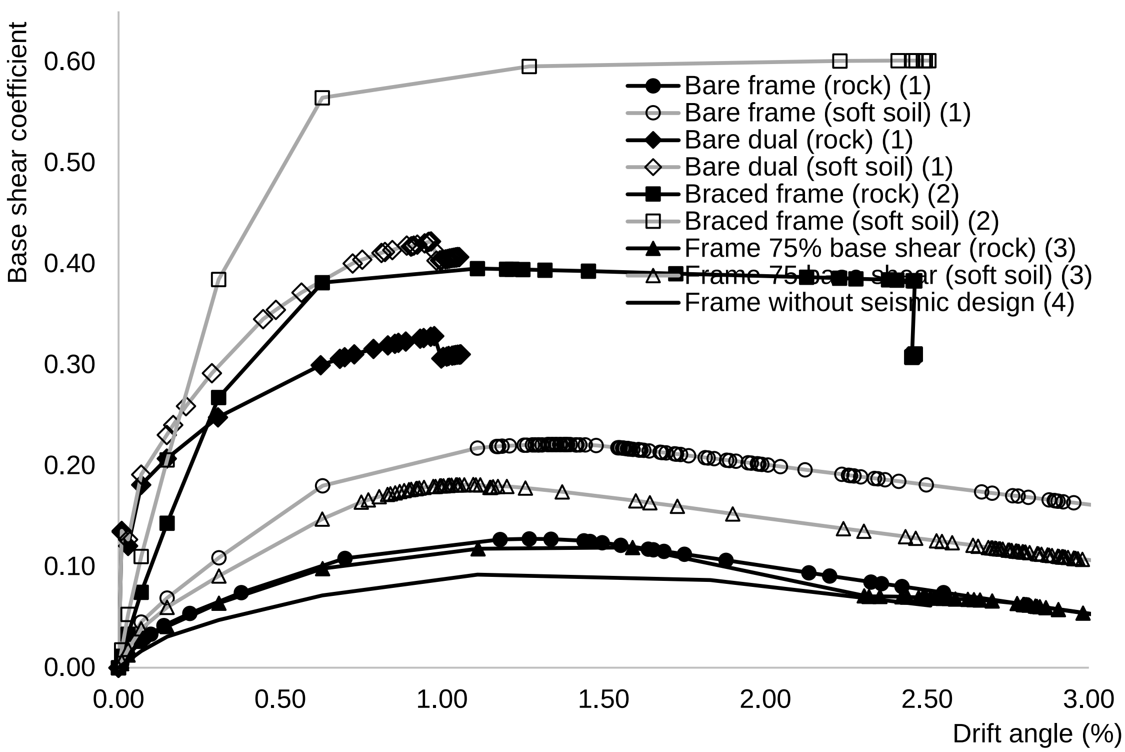

Fig. 4 – Capacity curves of the 3-story buildings (base shear coefficient vs. drift angle)

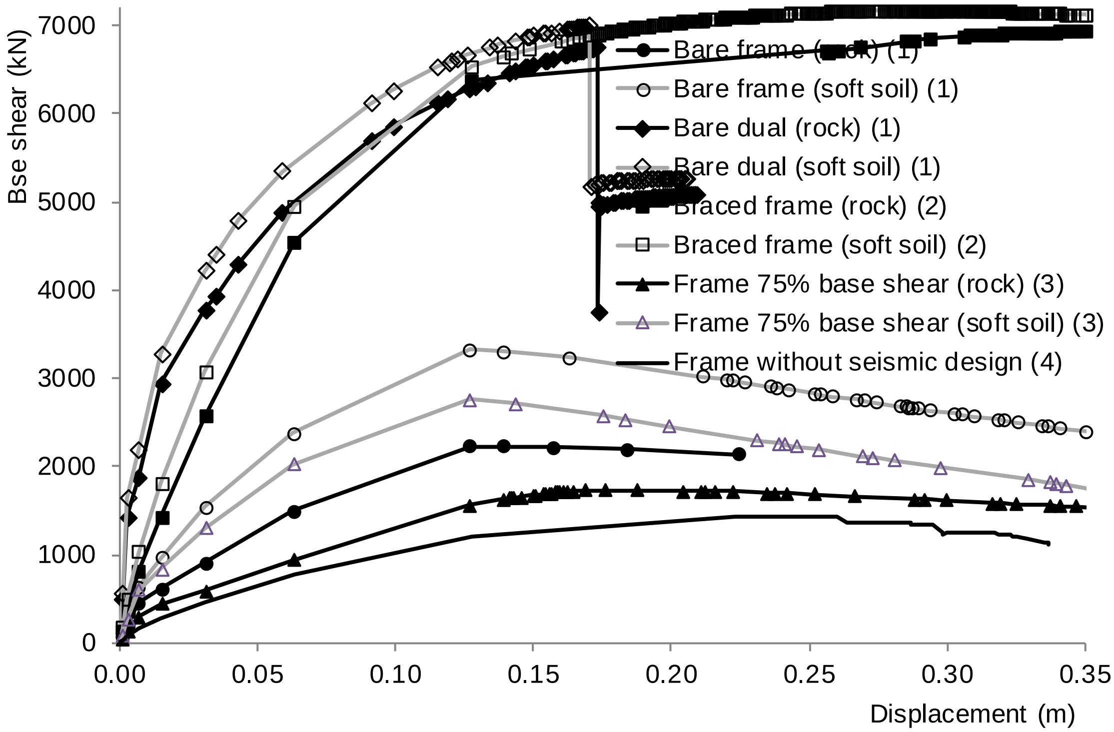

Fig. 5 – Capacity curves of the 5-story buildings

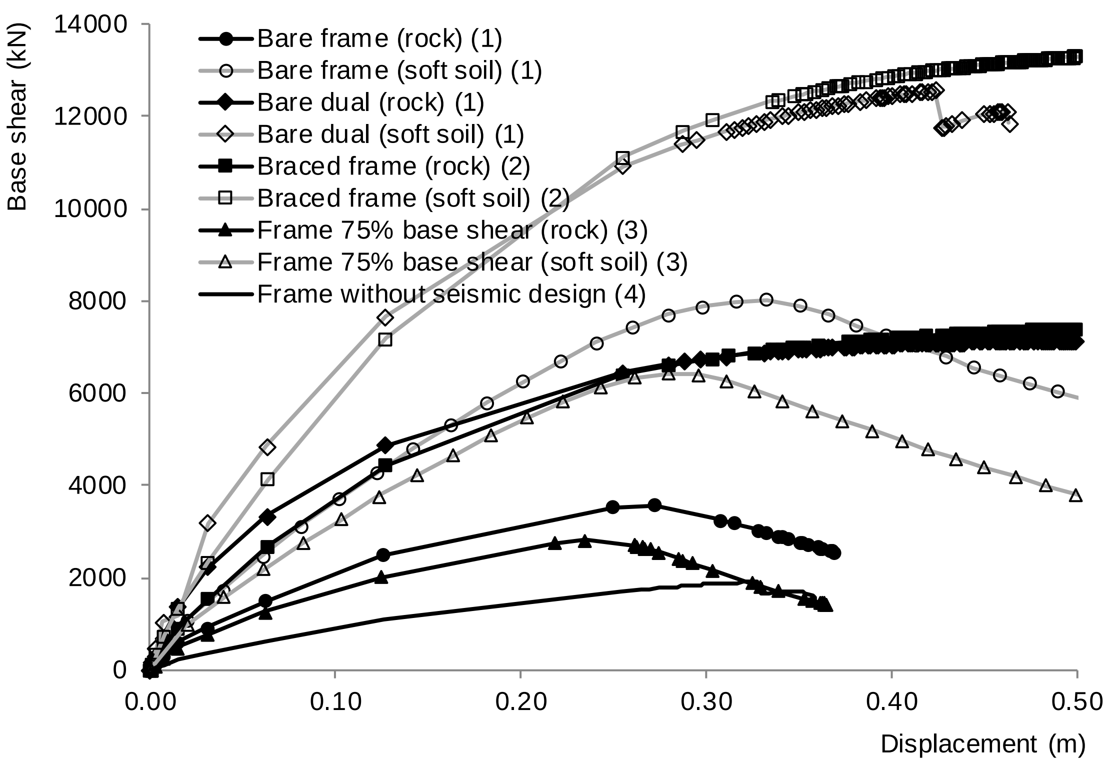

Fig. 6 – Capacity curves of the 10-story buildings

Fig. 3, Fig. 5 and Fig. 6 show a regular and expected behavior: the capacity of the buildings is higher for buildings with superior seismic demands, and dual (e.g. with structural walls) and braced buildings are stiffer than frame ones.

3. Seismic demand

Seismic demand is given as input and hysteretic energy (E_{I} and E_{H}) expressed in terms of equivalent velocities V_{E} and V_{D} according to $V_{\mathrm{E}} = \sqrt{2\,E_{\mathrm{I}}/m}$ and $V_{\mathrm{D}} = \sqrt{2\,E_{\mathrm{H}}/m}$, where m is the mass of the building. For practical energy-based earthquake-resistant design, V_{E} is obtained from available design energy spectra, and V_{D} is estimated from V_{E} through empirical expressions of the ratio V_{D} / V_{E}: V_{D} = V_{E} (V_{D} / V_{E}). Since design spectra are commonly derived after an important number of representative strong seismic ground motions, this strategy can provide an adequate level of safety. Among other researchers, [17] proposed design energy input spectra for moderate seismicity regions and [18] and [19,20] proposed design energy input spectra for moderate-to-high seismicity regions based on Colombian and on Turkish records, respectively. These V_{E} input energy spectra depend on the soil characteristics, the seismic design acceleration, the magnitude of the expected earthquakes and the type of seismic input (relevance of velocity pulses); conversely, they do not depend neither on the mass nor on the damping parameters. Moreover, except in the short period range, the V_{E} spectra are also independent on the assumed hysteretic constitutive law. A number of researchers [17-24] have derived empirical expressions of the ratio V_{D} / V_{E}; such expressions depend on the soil type, the structural damping, the fundamental period of the structure, and the displacement or cumulative ductility. The obtaining of input and hysteretic energy for the prototype buildings to be protected with energy dissipators (types 3 and 4 in subsection 2.1) is described next.

Input energy in terms of equivalent velocity (V_{E}). In this study, the seismic demand is derived after the design spectra proposed in [19,20]. These spectra depend on the soil characteristics (stiff / soft), the seismic design acceleration, the magnitude of the expected earthquakes ($M_{\mathrm{s}} \leq 5.5$ and $M_{\mathrm{s}} > 5.5$) and the type of seismic input (pulse-like / non pulse-like). As for the soil type, rock is broadly identified with stiff soil. Since the study in [19,20] is carried out assuming design acceleration 0.4 g, this fits in seismic zone 3 of Chile. Concerning the magnitude, given the high Chilean seismicity, it can be conservatively assumed that $M_{\mathrm{s}} > 5.5$. About the presence of velocity pulses, Chilean seismicity arises mainly from the subduction of the Nazca plate under the South American plate; since velocity pulses are more common in strike-slip mechanisms, the expected accelerograms will be mainly non pulse-like. For stiff and soft soil conditions, the V_{E} spectra proposed in [19,20] are shown in Fig. 7.a and Fig. 7.b, respectively. For linear analyses ($\mu = 1$, μ being the displacement ductility), spectra in Fig. 7 contain an initial linearly growing branch in the short period range, a plateau in the mid period range and a descendant branch in the long period range. The corner periods and the spectral ordinates for the plateau are indicated in Fig. 7; the exponents of the descending branches are 1.2 and 0.65 for stiff and soft soil, respectively. Except in the short period range, the input energy is a highly stable quantity [21] with respect to the hysteretic and damping parameters of the structure under consideration. Therefore, for nonlinear behavior (i.e. $\mu > 1$) the only required modification is an increase of the initial growing branch slope. This slope increase will result in a reduction of the lowest corner period; for instance, for $\mu = 20$ the ratio between both slopes is 1.41 and 1.56 for stiff and soft soil, respectively [19,20]. Therefore, the corner periods become 0.18 / 1.41 = 0.12 s (stiff soil) and 0.28 / 1.56 = 0.18 s (soft soil), as sown in Fig. 7. Both the linear and nonlinear spectra are characteristic, i.e. correspond to the 95% percentile, and are referred to 475 years return period. The values of V_{E} for the corresponding prototype buildings are obtained replacing the fundamental periods in Table 1 in the spectra in Fig. 7; these values are listed in Table 3. Noticeably, all the periods lie in the plateau (mid periods range).

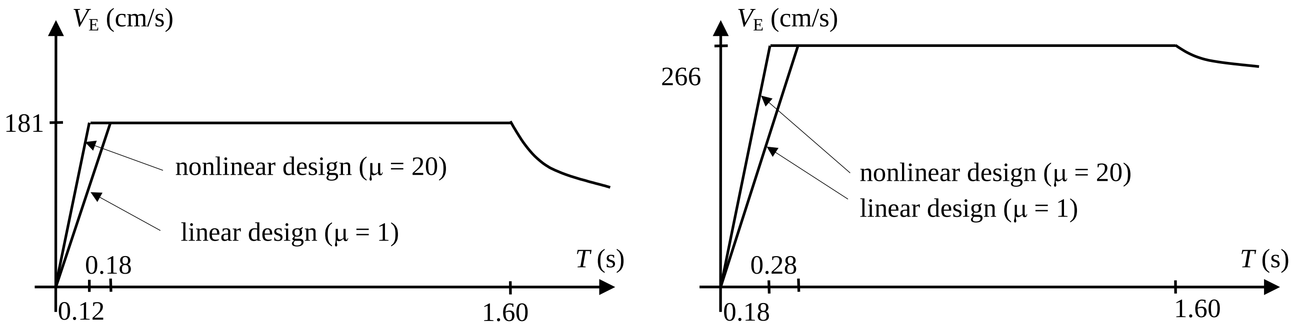

(a) Linear/nonlinear spectrum for stiff soil (b) Linear/nonlinear spectrum for soft soil

Fig. 7 – Input energy design spectra [19,20]

Hysteretic energy (E_H). V_D spectrum is commonly obtained by multiplying the V_E spectrum by a convenient value of the V_D / V_E ratio; such ratio depends mainly on the damping factor ζ, the displacement ductility μ and the building fundamental period T_F. References [19,20] contain linear regression studies providing average expressions V_D / V_E = $a\ T_F + b$ where coefficients a and b depend on ζ and μ. The hysteretic energy can be obtained after the equivalence equation $V_D = \sqrt{2\ E_H/m}$. In this study, coefficients a and b are selected for ζ = 0.05 and μ = 10: for both rock and soft soil, a = 0.88 and b = – 0.054 [19,20]. These values on ζ and μ are chosen as to correspond to average conditions. Noticeably, a more accurate analysis would require an iterative process in terms of ductility demand; however, it should emphasized that, for values of μ higher than approximately 5, ratio V_D / V_E is rather insensitive to that parameter. The selected values of V_D / V_E ratio re listed in Table 3.

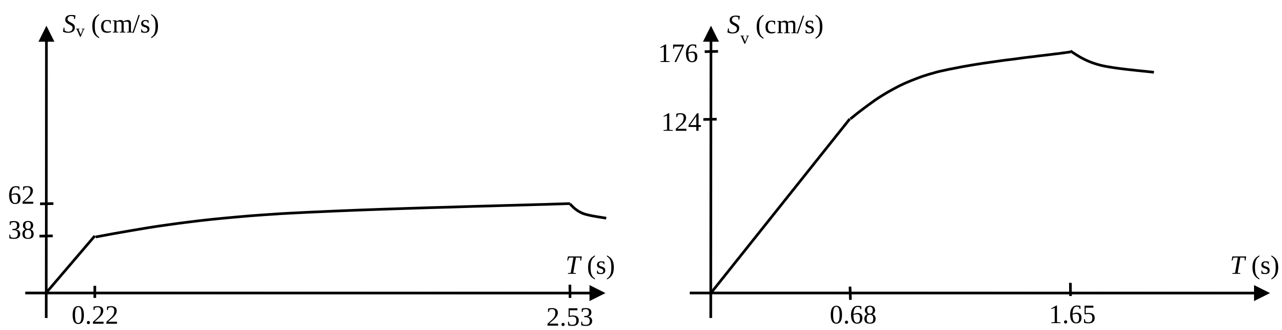

(a) Spectrum for rock / stiff soil (b) Spectrum for soft soil

Fig. 8 – Hysteretic energy design spectra obtained after the Chilean code [3]

This seismic demand in terms of hysteretic energy can be coarsely compared with the requirements of the Chilean code [3]. The comparison relies on the loose equivalence between the hysteretic energy V_D and the pseudo-velocity spectrum [21], obtained by multiplying the pseudo-acceleration spectrum by $T / 2\,\pi$. Acceleration spectral ordinates are derived after the design spectrum described in article 13 of the Chilean code. This spectrum is similar to those of mayor design codes and consists of a linear ascending branch ($T_a \le T \le T_b$), a plateau ($T_b \le T \le T_c$), a descending branch with exponent p ($T_c \le T \le T_d$) and a faster descending branch with exponent – 2 ($T_d \le T$). For rock / soft soil, T_a = 0, T_b = 0.13 / 0.37 s, T_c = 0.22 / 0.68 s, T_d = 2.53 / 1.65 s, p = 0.8 / 0.6. Comparison with the fundamental periods listed in Table 1 shows that most of the periods lie in the first descending branch (plateau of the velocity spectrum, mid periods range). The spectral ordinate for zero period is A_0, the plateau ordinate is $\alpha_A\ A$, the equation for the first descending branch is $(2 / \pi\ T^p)\ \alpha_V\ V$, and the equation for the second descending branch is $(4 / \pi^2\ T^2)\ \alpha_D\ D$. For rock / soft soil, $\alpha_A\ A$ = 1087 / 1142, $\alpha_V\ V$ = 51.5 / 144 s, and $\alpha_D\ D$ = 25 / 50. Fig. 8 displays the velocity spectra derived after the Chilean code [3]; for simplicity, in the range of very shorts periods ($T \le T_b$), spectra are represented with a linear branch. The resulting values of hysteretic energy are listed in Table 3; the buildings that were designed without any seismic consideration (type 4, subsection 2.1) are considered to be founded on soft soil.

Table 3 displays the energy demands on the buildings to be protected with energy dissipators. As in Table 1 and Table 2, numbers in parenthesis (3 and 4) correspond to the list in subsection 2.1.

Table 3 – Input and hysteretic(*) energy demand for the prototype buildings

No. of stories	Frame for 75% of base shear (3)								Frame without seismic design (4)			
	Rock				Soft soil							
	V_E (cm/s)	E_H (kNm)	V_D / V_E	E_H (kNm)	V_E (cm/s)	E_H (kNm)	V_D / V_E	E_H (kNm)	V_E (cm/s)	E_H (kNm)	V_D / V_E	E_H (kNm)
3	181	1443	0.854	1053 (87)	266	3396	0.856	2489 (525)	266	3163	0.847	2317 (620)
5	181	2633	0.837	1845 (195)	266	6187	0.844	4407 (1316)	266	5360	0.838	3818 (1274)
10	181	5841	0.804	3776 (541)	266	13820	0.820	9294 (4435)	266	11740	0.732	7893 (4139)

(*) Values in parenthesis correspond to the prescriptions of current Chilean code [3]

In Table 3, comparison between the hysteretic energy predicted by the Chilean code [3] grossly underestimates the demand obtained after [19,20]. The difference is particularly relevant for short buildings and for rock.

4. Damping system

4.1 Overall description

The proposed damping system consists in using additional bracing systems and installing hysteretic energy dissipators in between these elements and the main structure, as indicated in Fig. 1.a through Fig. 1.c. The solution using chevron braces (Fig. 1.a) is considered next. As shown in Fig. 1, devices are installed in all the floors; this guarantees an even behavior along building height (vertical uniformity). Aiming for plan symmetry and torsional strength, a device is placed in each of the four façades. Fig. 9 depicts the layout of devices in each floor. Noticeably, dissipators can be freely moved along their façades without disturbing plan symmetry and torsional strength.

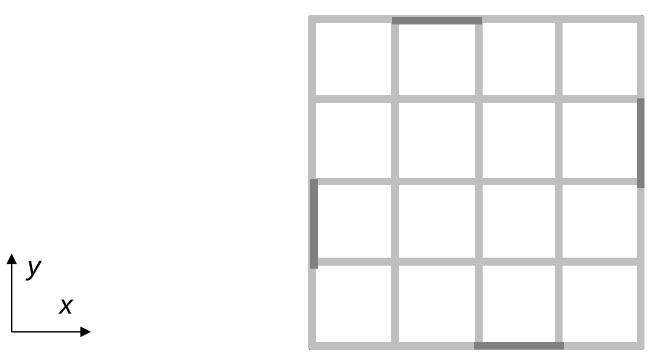

Fig. 9 – Plan distribution of dissipative devices

4.2 Hysteretic dissipators

Since the final goal of this research is to promote the massive use of hysteretic energy dissipators for seismic protection of vulnerable buildings in Chile, no specific recommendations for any specific device are given. For instance, the devices that were installed in the Titanium building might be adequate. The hysteretic behavior of any dissipator is characterized by three major parameters: yielding force, initial (elastic) stiffness and ratio between tangent (plastic) and initial stiffness.

4.3 Design of the dissipative devices

The energy that can be dissipated in the whole building in a given direction cannot be obtained by merely adding the capacities of each story; it depends on the distribution, among the different stories, of the dissipated energy and on the accidental eccentricities between their centers of mass and rigidity. To cope with this issue, a number of formulations to select the variation, along the building height, of the design stiffness and yielding forces of the steel members have been proposed; in this paper, the approach in [25] is considered. This formulation aims to obtain a rather uniform distribution of the cumulative ductility η in each level along the building height. The yielding shear force in the *i*-th floor (V_{yi}) is normalized with respect to the weight above that floor:

$$\alpha_{\mathrm{i}} = \frac{V_{\mathrm{yi}}}{\sum_{\mathrm{j=i}}^{\mathrm{N}} W_{\mathrm{j}}} \tag{1}$$

In equation (1), W_{j} is the weight of the *j*-th floor and *N* is the number of floors. This formulation considers the influence of the vertical distribution of the lateral stiffness of the main structure. The variation of α_{i} obeys to an exponential equation:

$$\frac{\alpha_{\mathrm{i}}}{\alpha_1} = \exp\left[\left(1 - 0.02\frac{k_1^{\mathrm{t}}}{k_{\mathrm{N}}^{\mathrm{t}}} - 0.16\frac{T_{\mathrm{F}}}{T_{\mathrm{G}}}\right)\frac{i-1}{N} - \left(0.5 - 0.05\frac{k_1^{\mathrm{t}}}{k_{\mathrm{N}}^{\mathrm{t}}} - 0.3\frac{T_{\mathrm{F}}}{T_{\mathrm{G}}}\right)\left(\frac{i-1}{N}\right)^2\right] \tag{2}$$

In equation (2), $k_{\mathrm{i}}^{\mathrm{t}}$ is the lateral stiffness of the *i*-th floor, T_{F} is the fundamental period of the building in the direction under consideration and T_{G} is the corner period of the V_{E} design spectrum (Fig. 7); T_{G} separates initial and horizontal branches.

5. Conclusions

This paper presents the preliminary steps of a research aiming to promote the mass use of hysteretic energy dissipators for seismic protection of vulnerable buildings in Chile. In this work, a number of representative prototype RC buildings are selected and designed according the current Chilean codes. The behavior of these buildings is analyzed in terms of modal parameters and capacity curves (after pushover analyses). The seismicity is characterized in terms of input and hysteretic energy; using this information, the optimal design parameters of the dissipative devices are obtained.

6. Acknowledgements

This work has received financial support from Spanish Government under projects BIA2014-60093-R and CGL2015-6591. These supports are gratefully acknowledged.

7. References

[1] Mata P, Barbat AH, Oller S, Boroschek R, (2008): Constitutive and Geometric Nonlinear Models for the Seismic Analysis of RC Structures with Energy Dissipators. *Archives of Computational Methods in Engineering*, **15** 489-539.

[2] Mata P, Barbat AH, Oller S, Boroschek R, (2009): Nonlinear seismic analysis of RC structures with energy dissipating devices. *International Journal for Numerical Methods in Engineering*, **78** 1037-1075.

[3] NCh 433 (2011): *Diseño Sísmico de Edificios*, Ministerio de Vivienda y Urbanismo de la República de Chile.

[4] ASCE/SEI 7-10 (2010): *Minimum Design Loads for Buildings and other Structures*, American Society of Civil Engineers.

[5] NCh 1537 (2009): *Diseño estructural de edificios - Cargas permanentes y sobrecargas de uso*, Ministerio de Vivienda y Urbanismo de la República de Chile.

[6] NCh 3171 (2010): *Diseño estructural Disposiciones generales y combinaciones de cargas*, Instituto Nacional de Normalización de Chile.

[7] NCh 430 (2011): *Hormigón armado - Requisitos de diseño y cálculo*, Ministerio de Vivienda y Urbanismo de la República de Chile.

[8] ACI 318-14 (2014): *Building Code Requirements for Structural Concrete*, American Concrete Institute.

[9] ASTM A36/A36 M-08 (2008): *Standard specification for carbon structural steel*.

[10] EN-1993 (2005): *Design of steel structures*, European Committee for Standardization.

[11] Seismosoft (2016). SeismoStruct v7 – *A computer program for static and dynamic nonlinear analysis of framed structures*, available from http://www.seismosoft.com.

[12] Paulay T, Priestley MJN (1992): *Seismic Design of Reinforced Concrete and Masonry Buildings*, John Wiley.

[13] EN-1992 (2004): *Design of concrete structures*, European Committee for Standardization.

[14] Spacone E, Filippou FC, Taucer FF (1996): Fibre Beam-Column Model for Nonlinear Analysis of R/C Frames: Part I. Formulation, *Earthquake Engineering & Structural Dynamics*, **25** 711-725.

[15] Neuenhofer A, Filippou FC (1997): Evaluation of nonlinear frame finite-element models, *Journal of Structural Engineering* **123**(7) 958-966.

[16] Imbsen CC (2002): XTRACT Software. Cross-Section Analysis Program for Structural Engineers. 2.6.2 *Imbsen and associates, Inc*.

[17] Benavent-Climent A, Pujades L, López Almansa F (2002): Design energy input spectra for moderate seismicity regions. *Earthquake Engineering & Structural Dynamics*. **31**:1151-1172.

[18] Benavent-Climent A, López Almansa F, Bravo González DA (2010). Design energy input spectra for moderate-to-high seismicity regions based on Colombian earthquakes. *Soil Dynamics & Earthquake Engineering*. **30**(11):129-1148.

[19] Yazgan U (2012): *Proposal of energy spectra for earthquake resistant design based on Turkish registers*. Doctoral Dissertation. Technical University of Catalonia.

[20] López Almansa F, Yazgan U, Benavent-Climent A (2013). Design energy input spectra for high seismicity regions based on Turkish registers. *Bulletin of Earthquake Engineering*. **11**(4):885–912.

[21] Akiyama H (1985): *Earthquake-resistant limit-state design for buildings*, University of Tokyo Press.

[22] Kuwamura H, Kirino Y, Akiyama H (1994): Prediction of earthquake energy input from smoothed Fourier amplitude spectrum, *Earthquake Engineering and Structural Dynamics* **23**:1125-1137.

[23] Fajfar P, Vidic T (1994): Consistent inelastic design spectra: hysteretic and input energy, *Earthquake Engineering and Structural Dynamics* **23**:523-537.

[24] Decanini LD, Mollaioli F (2001): An energy-based methodology for the seismic assessment of seismic demand, *Soil Dynamics and Earthquake Engineering* **21**:113-137.

[25] Benavent-Climent A (2011): An energy-based method for seismic retrofit of existing frames using hysteretic dampers. *Soil Dynamics & Earthquake Engineering*, **31**, 1385-1396.